Carbohydrate Polymers 106 (2014) 84–93

Contents lists available at ScienceDirect

Carbohydrate Polymers

journal homepage: www.elsevier.com/locate/carbpol

Characterization and properties of carboxymethyl cellulose hydrogels crosslinked by polyethylene glycol

Hiroyuki Kono*

Department of Science and Engineering for Materials, Tomakomai National College of Technology, Nishikioka 443, Tomakomai, Hokkaido 059 1275, Japan

ARTICLE INFO

Article history:
Received 19 December 2013
Received in revised form 31 January 2014
Accepted 5 February 2014
Available online 14 February 2014

Keywords:
Biodegradable hydrogel
Carboxymethyl cellulose
Polyethylene glycol
Protein adsorption
Protein release.

ABSTRACT

Novel hydrogels were prepared from carboxymethyl cellulose (CMC) sodium salt by crosslinking with polyethylene glycol diglycidyl ether (PEGDE). The detailed structures of the hydrogels were determined via FTIR and solid-state NMR spectroscopic analyses. Increasing the feed ratio of PEGDE to CMC in the reaction mixture led to an increase in the crosslinking degree, which enhanced the physical strength of the hydrogels. The hydrogels exhibited enzyme degradability, and after 3 days of incubation with cellulase, 62–28 wt% of the CMC in the hydrogel was degraded under the conditions employed in this study. In addition, the hydrogels exhibited protein adsorption and release abilities, and the amounts of proteins adsorbed on the hydrogels and the release profile of the proteins depended on the protein sizes and crosslinking degree of the hydrogels. These unique properties might enable the use of CMC-based hydrogels as drug delivery system carriers for protein-based drugs if the biological safety of the hydrogel can be verified.

1. Introduction

Carboxymethylcellulose sodium salt (CMC), obtained from the reaction of the hydroxyl groups of the anhydroglucose units (AGUs) of cellulose with chloroacetic acid, is an important water-soluble cellulose ether used in food, cosmetics, and paints as a viscosity modifier, thickener, emulsion stabilizer, and water-retention agent. CMC also has tremendous potential for use in pharmaceutical products including site-specific or controlled-release drug delivery system carrier matrices due to its high biocompatibility, biodegradability, and low immunogenicity (Colombo, Bettini, Sabti, & Peppas, 2000; Ugwoke, Kaufmann, Verbeke, & Kinget, 2000). Crosslinked CMC has also been accomplished with the use of bifunctional crosslinking agents such as epichlorohydrin (Chang, Duan, Cai, & Zhang, 2010), diepoxy (Lin, Kumar, Rozman, & Noor, 2005; Rodŕiguez, Alvarez-Lorenzo, & Concheiro, 2003; Kono, Onishi, & Nakamura, 2013), and dicarboxylic acid compounds (Akar, Antinişk, & Seki, 2012). Crosslinked CMC generally absorbs large amounts of water, and swells to form hydrogels with excellent physical properties and dynamic viscoelasticities (Nerurkar, Elliott, & Mauck, 2010). These CMC-based hydrogels were recently investigated for their use in wound dressing, drug delivery, agriculture, and sanitary pads, as well as for trans-dermal systems, dental materials, implants, injectable polymeric systems, ophthalmic applications, and hybrid-type organs (Sannino, Demitri, & Madaghiele, 2009; Saha, Saarai, Roy, Kitano, & Saha, 2011).

Among the various chemical crosslinking agents for CMC, epichlorohydrin (ECH) is the most popular and extensively used reagent to produce hydrogel materials because ECH is a strong etherification agent toward the hydroxyl group (Chang, Duan, Cai, & Zhang, 2010). The reaction of CMC with ECH in concentrated solutions of aqueous sodium hydroxide (NaOH) results in the formation of diether crosslinks between the hydroxyl groups of CMC and ECH to form a hydrogel (Ali Hebeish, Hashem, Abd El-Hady, & Sharaf, 2013; Yang, Fu, Liu, Zhou, & Li, 2011). However, ECH produces a large amount of poisonous and carcinogenic byproducts under strong alkaline conditions (Wester, van der Heijden, Bwiisschop, & van Esch, 1985). Other groups obtained similar CMC-based hydrogels with the use of ethylene glycol diglycidyl ether (EGDE) as a crosslinker (Lin et al., 2005; Rodŕiguez et al., 2003). It

Abbreviations: AGU, anhydroglucose unit; BPA, bisphenol A; BSA, bovine serum albumin; CMC, carboxymethyl cellulose; CD, cyclodextrin; DP, degree of polymerization; DD/MAS, dipolar-decoupled/magic angle spinning; DOSY, diffusion-ordered spectroscopy; DSS, 4,4-dimethyl-4-silapentane-1-sulfonic acid; ECH, epichlorohydrin; EGDE, ethylene glycol diglycidyl ether; FTIR, Fourier transform infrared spectroscopy; pI, isoelectric point; Mw, molecular weights; NMR, nuclear magnetic resonance; PBS, phosphate-buffered saline; PEG, polyethylene glycol; PEGDE, polyethylene glycol diglycidyl ether; SEM, scanning electron microscopy; SPINAL64, small phase incremental alternation with 64 steps; NaOH, sodium hydroxide.

* Tel.: +81 144 67 8036; fax: +81 144 67 8036.
E-mail address: kono@sem.tomakomai-ct.ac.jp

http://dx.doi.org/10.1016/j.carbpol.2014.02.020
0144-8617/

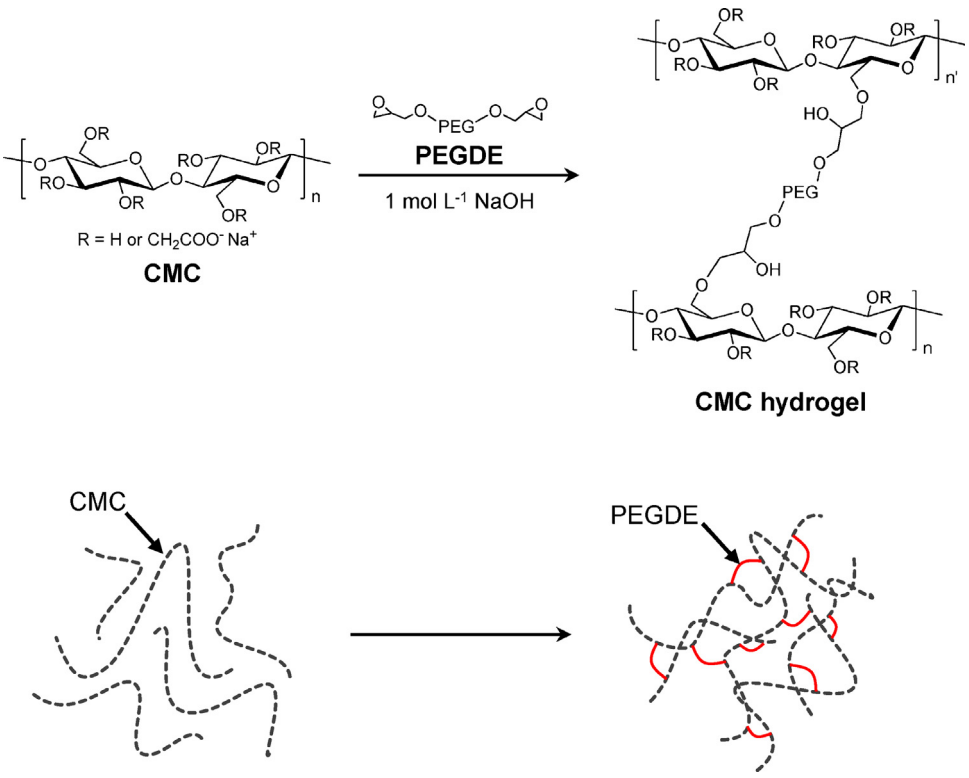

Fig. 1. Scheme for CMC hydrogel synthesis via crosslinking of CMC with PEGDE (top), and schematic illustration of the formation of the CMC hydrogel from CMC and PEGDE (bottom). In the top figure, the linkage positions of CMC and PEGDE are shown at C6 of AGU in CMC. PEGDE can also react with the hydroxyl groups of the other position of CMC and PEGDE to form cross-linked linkages. This possibility was omitted in this figure.

was recently reported that cyclodextrin (CD)-grafted CMC hydrogel beads were prepared from a mixture of CMC and β-cyclodextrin (β-CD) by the crosslinking reaction with ethylene glycol diglycidyl ether (Kono et al., 2013c). The CD-CMC hydrogels showed excellent water absorption as well as a high adsorption capacity toward bisphenol A (BPA) in water.

Polyethylene glycol (PEG) is a synthetic polyether that is readily available in a range of molecular weights. The polymer is amphiphilic and soluble in water as well in many organic solvents including ethanol, acetone, toluene, and chloroform (Bailey & Koleske, 1991; Bailey & Koleske, 1976). This polymer has been found to be nontoxic and is approved by the U.S. Food and Drug Administration for use as an excipient or as a carrier in different pharmaceutical formulations, foods, and cosmetics (Fuertges & Abuchowski, 1990). In addition, most PEGs with molecular weights (Mw) < 1,000 are known to be rapidly removed from the human body (Working, Newman, Johnson, & Cornacoff, 1997), which contributes to their wide use in biomedical research, drug delivery, tissue engineering scaffolds, surface functionalization, and so forth (Torchilin, 2002; Craig, 2002).The wide range of available end-groups, e.g., azide, biotin, thiol, carboxyl acid, hydroxyl, and epoxy-functionalized PEGs, also enhances the wide spread use of PEGs in biomedical and biomaterial research (Zalipsky, 1995).

Therefore, the preparation of a novel biodegradable hydrogel from CMC with polyethylene glycol diglycidyl ether (PEGDE) as a crosslinking agent, as shown in Fig. 1, is described here. By changing the feed ratio of PEGDE to CMC, we prepared a series of CMC-based hydrogels, and characterized the structure of the hydrogels using FTIR, solid-state NMR, and scanning electron microscopy (SEM). The viscoelasticities of the swelled hydrogels were characterized by using a rheometer. In addition, we also evaluated the protein adsorption and release properties of the CMC hydrogels using lysozyme and bovine serum albumin (BSA) as model proteins.

2. Experimental

2.1. Materials

Pharmaceutical grade CMC was kindly supplied by CP Kelco Co., Ltd. (Finland). PEGDE was purchased from Sigma–Aldrich Co. (USA). The weight-average molecular weight (Mw) and degree of substitution of the starting material CMC, and average degree of polymerization (DP) of PEGDE were estimated by solution-state NMR spectroscopic analysis before use, and the procedure is described below (see Section 2.3). Deuterium oxide (D_2O; 99.9% isotopic purity) containing 4,4-dimethyl-4-silapentane-1-sulfonic acid (DSS) as an internal standard was purchased from Sigma-Aldrich Co. (USA). *Trichoderma viride* Cellulase (ONOZUKA R-10) was purchased from Yakult Pharmaceutical Co. Ltd. (Japan). Protein assay kit II was purchased from Bio-Rad Laboratories Co. (USA). BSA and egg white lysozyme were purchased from Wako Pure Chemicals Co. (Japan). All other chemicals were purchased from Kanto Chemicals (Japan) and Wako Pure Chemicals (Japan), were of reagent grade, and were used as received.

2.2. Preparation of hydrogels

A series of five CMC hydrogels (entries **1**–**5**) were prepared from CMC with PEGDE. A typical procedure to prepare the CMC hydrogel was performed as follows: 5.0 g of CMC (23 mmol for monomeric unit) was completely dissolved in 100 mL of 1.5 mol L^{-1} aqueous NaOH solution, and 0.50 g of PEGDE (1.1 mmol) was subsequently added to the solution with stirring at 300 rpm using a Teflon impeller at 25 °C. After 10 min, the crosslinking reaction was performed at 60 °C with stirring at 300 rpm for 3 h. The reaction mixture was washed twice with a solution of 1:1 (v/v) deionized water and ethanol, and the resultant reaction mixture was dialyzed

Table 1
Reaction conditions, yields, and structural parameters of CMC hydrogels.

Entry	Initial additive amounts for preparation		Yields [a]	Integrated value of ^{13}C resonances [b]		Structural parameters	
	CMC	PEGDE		I_{CO}	I_{others}	n_{PEG} [c]	$n_{PEG}{}^{-1}$ [d]
1	5.0 g	0.5 g	5.0 (91%)	0.67	6.80	6.4×10^{-3}	156
2	5.0 g	1.0 g	5.1 (85%)	0.67	6.93	12.7×10^{-3}	79
3	5.0 g	1.5 g	5.8 (89%)	0.67	7.15	23.5×10^{-3}	43
4	5.0 g	2.0 g	6.0 (86%)	0.67	7.28	29.9×10^{-3}	33
5	5.0 g	2.5 g	6.4 (85%)	0.67	7.41	36.6×10^{-3}	27
CMC				0.67	6.67		

[a] Yields (%) of each entry was determined by the following equation: (mass of hydrogel/g) × 100/(sum of mass of CMC and PEGDE/g) %
[b] Integrated values of I_{CO} and I_{others} were determined from the integration of the carbonyl carbon region (183–172 ppm) and the other carbon region (108–58 ppm) in each solid-state ^{13}C DD/MAS spectrum shown in Fig. S5, respectively. For all entries, I_{CO} was set to 0.67 which is the DS of the starting material CMC.
[c] Average number of the crosslinked PEGDE molecules per one AGU of CMC in each hydrogel.
[d] Average number of AGU of CMC per one PEGDE molecules crosslinked with CMC in each hydrogel.

with a dialysis membrane (M_W 12,000–13,000 cut) against distilled water. The dialyzed hydrogel was freeze-dried and subsequently screened through a 40 mesh sieve to obtain the white granular CMC hydrogel (entry **1**). Using a similar method to prepare the CDCMC hydrogels, the other CDCMC hydrogels (entries **2**–**5**) were prepared and the amounts of the CMC and PEGDE used for the preparation of these hydrogels are listed in Table 1. All hydrogels were stored in a desiccator under vacuum until the time of use.

2.3. Structural analysis

2.3.1. NMR spectroscopy

All NMR spectra were recorded on a Bruker AVIII spectrometer (Germany, ^1H frequency of 500.13 MHz and ^{13}C frequency of 125.13 MHz). Solution-state NMR spectra of PEGDE and CMC were obtained by use of a 2-channel 5 mm BBO probe incorporating a *z*-gradient coil. The measurement temperature for PEGDE and CMC was set to 300 K and 353 K, respectively. One drop of PEGDE or 3 mg of CMC dissolved in 0.6 mL of D_2O in a 5 mm NMR glass tube (Wilmad-Labglass Co, USA) was used for the NMR experiments. For the quantitative discussion, 1D inverse-gated ^1H-decoupled ^{13}C NMR spectra (Canet, 1976) of PEGDE and CMC were recorded by the use of Bruker's Biospin default pulse program. The excitation pulse for ^{13}C nuclei with a flip angle of 30°, data acquisition time, and repetition time were set to 15 μs, 2.71 s, and 30 s, respectively, and 256 scans for PEGDE and the 20,480 scans for CMC were collected. The ^{13}C chemical shifts of the NMR data were calibrated by assigning the methyl peak of DSS as 0 ppm. ^1H diffusion-ordered (DOSY) NMR spectrum of CMC was obtained at 300 K with the use of the bipolar pulsed field gradient longitudinal eddy delay with presaturation for the water suppression pulse sequence (Nilsson, 2009). Thirty-two spectra with 16 K data points were collected using 32 scans, with values for the duration of the magnetic field pulse gradients of 4 ms, diffusion times of 160 ms, and an eddy current delay of 5 ms. The pulse gradient was incrementally increased from 1 to 95% of the maximum gradient strength in a linear ramp. The spectra were first processed in the F2 dimension by standard Fourier transformation with subsequent baseline correction of the diffusion dimension processed by Bruker's Biospin Topspin software package (Version 3.0). The diffusion coefficient (D) of CMC was calculated by an exponential fitting of the data belonging to individual columns in a two-dimensional matrix. The diffusion coefficient D was obtained by measuring the signal intensity at more than one point of the spectra (Kono & Nakamura, 2013).

Solid-state dipolar-decoupled/magic angle spinning (DD/MAS) ^{13}C NMR spectra of the hydrogels were recorded at 25 °C with the use of a 4 mm dual-tuned MAS probe at a MAS frequency of 12.5 kHz. ^{13}C-excitation pulse length (flip angle of 30°), data acquisition time, and repetition time were set to 1.5 μs, 20 ms, and 30 s, respectively. During the data acquisition period, small phase incremental alternation with 64 steps (SPINAL 64) proton decoupling (Fung, Khitrin, & Ermolaev, 2000) was applied with a ^1H field strength of 100 kHz. The spectra were typically accumulated with 3,076 scans to achieve an acceptable signal-to-noise ratio. Chemical shifts of the ^{13}C spectra were calibrated based on the carbonyl carbon resonance of D-glycine at 176.03 ppm, which was used as an external reference.

2.3.2. FTIR spectroscopy

The FTIR spectra of the hydrogel beads were measured using a PerkinElmer Spectrum Two spectrometer (PerkinElmer Inc., USA). FTIR spectra were recorded after grinding the sample into a powder and mixing well with KBr powder. The powder mixture was compressed into a transparent disk and scanned from 4,000 to 500 cm^{-1} using an average of 16 scans, with a resolution of 1 cm^{-1}.

2.4. Morphological observation

SEM images of the cross-sectional structures of the swollen hydrogels were observed using the following sample preparation: after swelling in deionized water at 25 °C for 48 h, the hydrogels were carefully cut by a razor blade, frozen at −70 °C, and then the freeze-dried under vacuum until water was sublimed. SEM images of the swollen hydrogels were obtained by the use of a Hitachi TM3030 scanning electron microscope (Hitachi High-Technologies Co. Ltd., Japan) with a potential of 5 kV and without vapor deposition on the sample surface.

2.5. Rheological properties

The rheological behavior of the swelled hydrogel was evaluated in triplicate, using a Physica MCR 301 rheometer (Anton Paar GmbH, Austria) equipped with a Rheoplus 32 data analyzer, and fitted with a Peltier temperature control. A 50 mm rough surface cone-plate measuring geometry was used to prevent sample slippage. The temperature of all measurements was kept constant at 298 K. The gap and stain were set at 1.0 mm and 1.0%. Oscillatory shear responses (G′ or storage modulus, and G″ or loss modulus) were determined at 0.1 Pa over the frequency range of steady shear tests over a share rate range of 0.063–63 rad s^{-1}. The test conditions were inside the linearity range of the viscoelastic properties.

2.6. Water absorption and water-holding capacity

The water absorbency of the hydrogels was determined according to the tea-bag method of the Japan Industrial Standard, JIS K7223 (Kono & Fujita, 2012). A nylon-tea bag with dimensions of 50 × 100 mm was prepared from a 225 mesh nylon sheet using a

heat sealer. The hydrogel (100 mg) was placed into the tea bag, which was then immersed in pure water at 25 °C. After a certain amount of time, the tea bag was removed from the aqueous solution and the excess water was drained for 10 min. The weight of the tea bag including the swollen hydrogels (W_h) was measured, and the water absorbency was calculated using the following equation:

$$\text{Water absorbency} = (W_h - W_b - W_d)/W_d,$$

where W_b is the weight of the empty tea bag after the water treatment, and W_d is the weight of the dried superabsorbent hydrogel. As an external solution for determining the absorbency, 0.9 (w/v)% saline water was also employed. These absorbency measurements were taken for five samples of each hydrogel, and the average of the five values was plotted against the absorption time.

Water-holding capacity of the swelled hydrogels was determined by the following method: the nylon tea-bag containing hydrogel sample (100 mg) immersed in pure water at 25 °C for 3 days was placed in a KCL-2000A temperature and humidity testing chambers (EYELA Co. Ltd., Japan) whose temperature and humidity were precisely controlled at 25 °C and 40%, respectively. After a certain amount of time, the weight of the tea bag including the hydrogels was measured, and the water-holding capacity was determined using the following equation:

$$\text{Water-holding capacity}\,(\%) = (W_t - W_b - W_d) \times 100/(W_e - W_b - W_d),$$

where W_t is weight of the tea-bag including the swollen hydrogel at a certain time, and W_e is weight of tea bag including the swollen hydrogel at initial state. These water-holding measurements were taken for five samples of each hydrogel, and the average values were plotted against time.

2.7. Cellulase degradation

Before performing the cellulase degradation test, *Trichoderma viride* cellulase ONOZUKA R-10 was purified according to the following method at 4 °C: the cellulase powder (10 g) was dissolved in 250 mL of 50 mM acetate buffer, pH 5.0. Ground, powdered $(NH_4)_2SO_4$ (180 g) was added to the solution to give 90% saturation. The precipitate was collected by centrifugation, desalted by ultrafiltration using a Q0100 filter (Advantec Co. Ltd., Japan), and then lyophilized (Kono & Zakimi, 2013). The obtained cellulase powder was used for the biodegradation of the hydrogels. The protein mass of cellulase was determined by use of the Bio-Rad protein assay kit (Bio-Rad Co.) with BSA as a standard (Zor & Selinger, 1996). Cellulase activity was measured using CMC as a substrate. A total of 10 mL of the reaction mixture containing 9 mL of 1% (w/v) CMC in 50 mM sodium acetate buffer (pH 5.0), and 10 mg of the purified cellulase dissolved in 1 mL of the same buffer solution was incubated at 40 °C. After 30 min, the amount of reducing sugars in the mixture was measured by the dinitrosalicylic acid method (Miller, Blum, Glennon, & Burton, 1960). One unit of cellulase activity was defined as the amount of enzyme liberating 1 μmol of reducing sugar per min.

The cellulase degradability test of the hydrogels was carried out according to the following procedure: 100 mg of the hydrogel sample was sufficiently soaked in 19 mL of 50 mM sodium acetate buffer for 1 day. Cellulase dissolved in 1 mL of the same buffer solution was added to the suspension to give a cellulase concentration of 10 units/mL. The mixture was incubated at 40 °C. After a certain amount of time, an aliquot (0.25 mL) was withdrawn from the mixture, and the amount of reducing sugars in the aliquot was determined by the method described above. The degradability of the hydrogels was determined using the following equation:

$$\text{cellulase-degradability}\,(\%) = (M_s - M_b) \times 100/M_s,$$

where M_s is the molar mass of AGU in the hydrogel before the degradation, and M_b is the molar mass of the reducing sugars liberated by the cellulase.

2.8. Protein adsorption and release properties

In the protein adsorption experiments, hen egg white lysozyme and BSA whose molecular weights are 14 kDa and 66 kDa, respectively, were used as model proteins. Lysozyme or BSA was dissolved in 7 mL of 20 mM phosphate-buffered saline (PBS) solution (pH 7.4) and 35 mg of the hydrogel was added to the protein-containing buffer. The adsorption experiments were then conducted in a thermostat-containing water bath at 25 °C for 24 h, with shaking at a rate of 120 rpm. At the end of the binding period, the mixture was centrifuged at 15,000 rpm for 2 min, and the protein-adsorbed hydrogel was obtained (Kono, Oeda, & Nakamura, 2013). The protein concentration of the supernatant was estimated at a wavelength of 280 nm using an Evolution 201 UV–vis spectrophotometer. The amount of protein adsorbed to the hydrogels was determined by the following equation:

$$\text{Protein adsorption}\,(\%) = \{[\text{Protein}]_{\text{init}} - [\text{Protein}]_{\text{sup}}\} \times 100/[\text{Protein}]_{\text{init}},$$

where $[\text{Protein}]_{\text{init}}$ and $[\text{Protein}]_{\text{sup}}$ are the initial protein concentration of PBS solution and the protein concentration of supernatant after protein adsorption, respectively.

The protein-adsorbed hydrogels were freeze-dried, and the resulting hydrogel was used for the protein release experiment. 10 mg of the freeze-dried hydrogel was added to 15 mL of a polypropylene tube containing 10 mL of 20 mM PBS solution (pH 7.4). The tube was placed into a thermostat-containing water bath (25 °C) with a shaking rate of 120 rpm. The protein release from the hydrogels was determined by applying the amounts of released and adsorbed protein to the following formula (Kono et al., 2013b):

$$\text{Protein release}\,(\%) = (\text{the amount of desorbed protein}) \times 100/(\text{the amount of adsorbed protein}).$$

3. Results and discussion

3.1. Characterization of starting materials of CMC and PEGDE

Before the preparation of the CMC hydrogel, the Mw and DP of PEGDE and CMC were characterized by NMR spectroscopic analysis. Fig. S1 shows the inverse-gated ^{1}H-decoupled ^{13}C NMR spectrum of PEGDE. Each carbon resonance was assigned previously (Harris, 1985); 71.4, 69.7, 51.5, and 44.9 ppm were assigned to methine carbons of the epoxide groups, methylene carbons of PEG, methylene carbon of the end units, and methylene carbons of the epoxide groups, respectively. In this figure, the sum of the integrations of the 71.4 ppm and 69.7 ppm lines was 7.2 when the intensity of the other carbon was 1. Therefore, the DP of the PEG moiety of PEGDE was determined to be 7.2 and the average Mw of PEGDE was 436.

The structure of the starting material CMC was determined from the quantitative ^{13}C NMR measurements of CMC, as shown in Fig S2. In the spectrum, the integral values of the carbonyl carbons appearing at 183–178 ppm and C1 of AGU appearing at 108–102 ppm were 0.67 and 1, respectively. Thus, the DS of CMC was revealed to be 0.67, and the average monomer Mw could be

estimated to be 216 (Kono, 2013). The ^{1}H DOSY spectrum of the CMC is shown in Fig. S3, where the ^{1}H chemical shift and diffusion coefficients (D) are represented orthogonal to each other. This bidimensional map clearly illustrates that the diffusion coefficient D of CMC was 2.63×10^{-11}. Nishinari et al. (1991) formulated the following equation between D and Mw of polysaccharides at 300 K using solutions containing pullulan standard samples of known molecular weight:

$$D = 8.2 \times 10^{-9}\,\mathrm{Mw}^{-0.49}(m^2\,s^{-1}).$$

In addition, some reports demonstrated that this equation could be applied to the Mw estimation of a wide range of water-soluble nonionic and anionic saccharides including mono-, oligo-, and polysaccharides (Viel, Capitani, Mannina, & Segre; 2003; Kono & Nakamura, 2013). By substituting the diffusion coefficients of CMC into the equation, the Mw of CMC was determined to be 123,000, indicating that the average DP of CMC was 569. Using these PEGDE and CMC, a series of CMC hydrogels were prepared.

3.2. Preparation of CMC hydrogels

As shown in Fig. 1, the preparation of the CMC hydrogels was performed in aqueous NaOH solution using PEGDE as an ether crosslinking agent. In this study, a series of five hydrogels (entries **1**–**5**) were prepared by varying the initial feed of PEGDE to CMC, as summarized in Table 1. In the crosslinking reaction, the transparent CMC solution became increasingly viscous soon after the addition of PEGDE, and the morphology of the mixture gradually changed from a solution to a gel after the onset of heating at 60 °C. After a reaction time of 3 h, a transparent gel was obtained, crushed, and thoroughly washed with a mixture of deionized water and ethanol. The resultant gel was dialyzed against a continuous stream of water for 3 days, dried under vacuum, and then screened through a 40 mesh sieve to obtain a white granular product. The yield of the series of CMC hydrogels ranged from 85–91% (Table 1).

3.3. Structure of CMC hydrogels

Fig. S4 shows the FTIR spectra of the starting material CMC and CMC hydrogels (entries **1**, **3**, and **5**). These spectra were normalized by the absorption of the carboxylate group at 1596 cm^{-1} (Kono et al., 2013c). With the exception of the band at 1,596 cm^{-1}, these spectra display common adsorption bands at 3396, 2918, 2874, 1417, 1323, and 894 cm^{-1}, which can be assigned to the stretching vibration of OH, asymmetric stretching vibration of the aliphatic CH_2, symmetric stretching vibration of CH_2, scissoring bending vibration of CH_2, bending vibration of CH, and the vibration of the α-(1 → 4) glucopyranose ring, respectively (Rozenberg, Loewenschuss, & Marcus, 1998; Kono et al., 2013c). The intensity of the bands at 2918, 2874, 1417, and 1323 cm^{-1} of the CMC hydrogels were obviously increased as compared to those of CMC, which indicated that the PEGDE reacted with CMC. In addition, intensity of those bands were enhanced with the increase in the feed amounts of PEGDE in the preparation of CMC hydrogels, while there was little change in the intensities of 894 cm^{-1} bands of these samples. Therefore, a high feed ratio of PEGDE prompted the crosslinking of CMC by PEGDE. In order to obtain more detailed and clear information about the molecular structure of CMC hydrogels, solid-state ^{13}C NMR measurements were performed.

Fig. 2 shows the solid-state ^{13}C NMR spectra of CMC and CMC hydrogel (entries **3**, **4**, **5**). In the spectrum of CMC, broad ^{13}C resonances at 178, 104, 83, 75, and 63 ppm were assigned to the carbonyl carbon, C1, C4, overlap of C2, C3, C5 and methylene carbons of carboxymethyl groups, and C6, respectively (Kono et al., 2013c). In the ^{13}C spectra of CMC hydrogels, a new resonance appearing

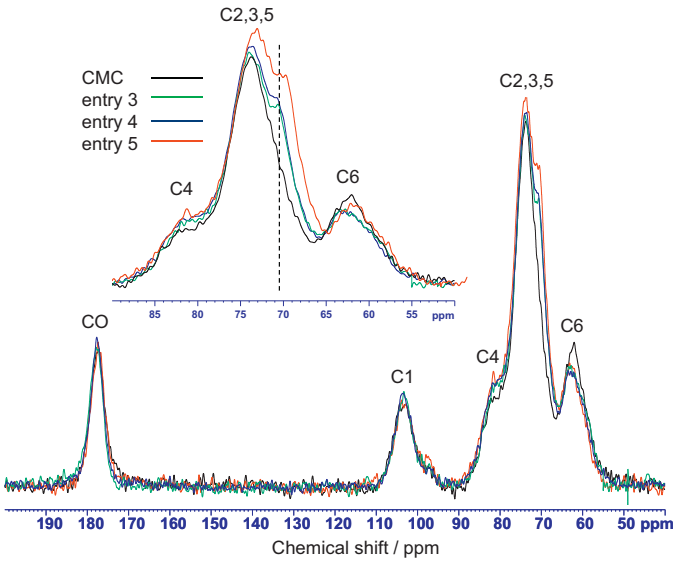

Fig. 2. Solid-state DD/MAS ^{13}C NMR spectra of CMC and CMC hydrogels (entries **3**–**5**). These spectra were normalized by the peak intensity of the carbonyl carbon at 178 ppm.

around 71 ppm was observed in addition to the resonances of CMC. Compared to the solution-state ^{13}C NMR spectrum of PEGDE (Fig. S1), the resonance at 71 ppm could be assigned to the methylene carbons of PEGDE crosslinked to CMC. Moreover, the methoxy carbon of the epoxide group in PEGDE whose chemical shift is 44.9 ppm (Fig. S1) could not be observed in the solid-state NMR spectra of CMC hydrogels. This indicates that the epoxy groups of PEGDE reacted with the hydroxyl groups of CMC to form the ester crosslink and that there was no graft form of PEG in the hydrogels.

To estimate the amounts of PEGDE crosslinked to CMC in these hydrogels, integration values of carbonyl carbons (I_{CO}) and the other carbon resonances (I_{others}) of each hydrogel were determined (Fig. S5). The I_{others} for each hydrogel when I_{CO} was set to 0.67 and is summarized in Table 1. A gradual increase of I_{others} with an increase in the feed amount of PEGDE to CMC in the preparation of the hydrogels was observed. From the I_{others} value for each hydrogel, the average number of the crosslinked PEGDE per one AGU of CMC, which was defined as crosslinking degree (n_{PEG}), could be determined by following equation:

$$n_{PEG} = (I_{others} - 6.67)/20.4,$$

where constants 6.67 and 20.4 were the carbon number of AGU of CMC and that of the average one PEGDE molecule, respectively. Therefore, the average number of AGU molecules of CMC per 1 unit of PEGDE could be calculated by the following equation:

$$(\text{the average number of AGU molecule of CMC per 1 unit of PEGDE}) = 1/n_{PEG}$$

These structural parameters for each hydrogel are also summarized in Table 1. From this data, it was clearly revealed that n_{PEG} increased with an increase in the feed ratio of PEGDE to CMC during the hydrogel preparation.

3.4. Water absorption and water-holding capacity

The white-colored granular CMC hydrogel absorbed water readily and formed transparent hydrogels upon soaking. Fig. 3(A) shows the time dependency of the absorbance of the hydrogels toward pure water. The maximum absorbency of the hydrogels

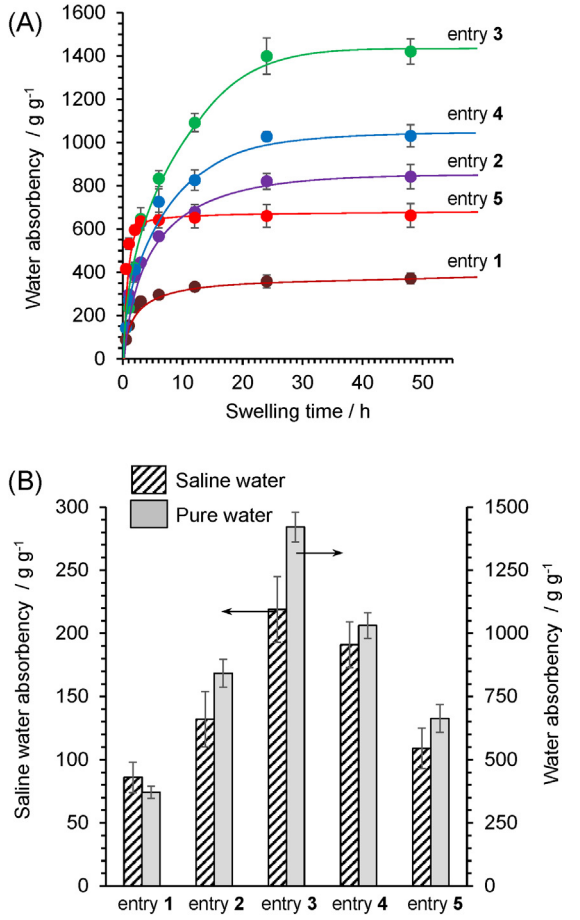

Fig. 3. (A) Time-dependence of the absorbency of CMC hydrogels toward pure water. (B) Absorbance of the CMC hydrogels toward pure and 0.9 (w/v)% saline waters after 72 h.

was reached within 48 h. Comparison of the hydrogel absorbencies shows that the absorbency increased with increasing n_{PEG} up to 23.5×10^{-3} (entry **3**), and that the highest absorbency was 1420 g/g-hydrogel. On the other hand, absorbency samples with higher n_{PEG} (entries **4** and **5**) decreased, which indicates that the expansion of hydrogels was suppressed by PEG molecules at high crosslinking degrees.

Fig. 3(B) shows the absorbencies of each hydrogel toward pure water and 0.9% saline water after 48 h. The absorbency of hydrogels toward saline water exhibited a similar trend as the absorbency toward pure water. In the case of saline water, however, the absorbency was drastically lowered to about 15–23% of the absorbency toward pure water. Absorption of water by ionic gels is generally influenced by the osmotic pressure caused by the difference in the mobile cation concentration between the gel (Kono, Fujita, & Oeda, 2013) and the saline solution. This reduces the osmotic pressure, thereby drastically lowering the absorbency of hydrogel.

After testing the absorbency, the tea-bag-containing hydrogels swollen by pure water were set on the temperature and humidity testing chambers at 25 °C and 40%, respectively. After a prescribed time, the weights of the tea bags including the hydrogels were measured, and the water-holding capacity for each hydrogel was estimated (Fig. S6). Each hydrogel released water from the gel inside with time. From the data, the release rate of water increased with lower n_{PEG}. This suggests that the hydrogels with a high crosslinking degree could keep water molecules in the gel network structures.

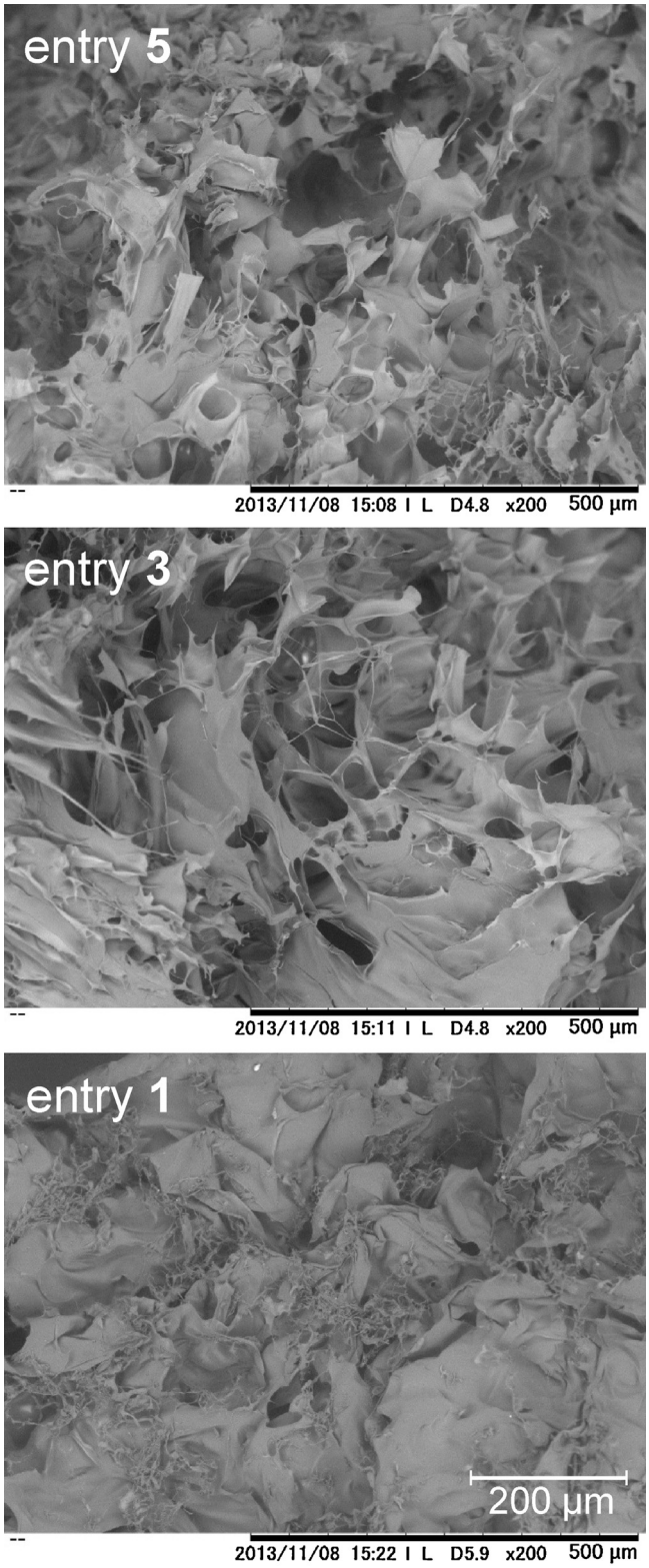

Fig. 4. SEM images of a cross-section of CMC hydrogels (entries **1**, **3**, and **5**).

To reveal the relationship between structure and water-holding capacity of the hydrogels with different n_{PEG}, SEM images of the cross-sections of the lyophilized hydrogels (entries **1**, **3**, **5**) were observed (Fig. 4). The porous structure could be observed in the cross-section surface of entries **3** and **5**, and the pore size of entry **3** was larger than that of entry 5. This indicates that entry **3** of $n_{PEG} = 23.5 \times 10^{-3}$ could swell a large amount of water, but the

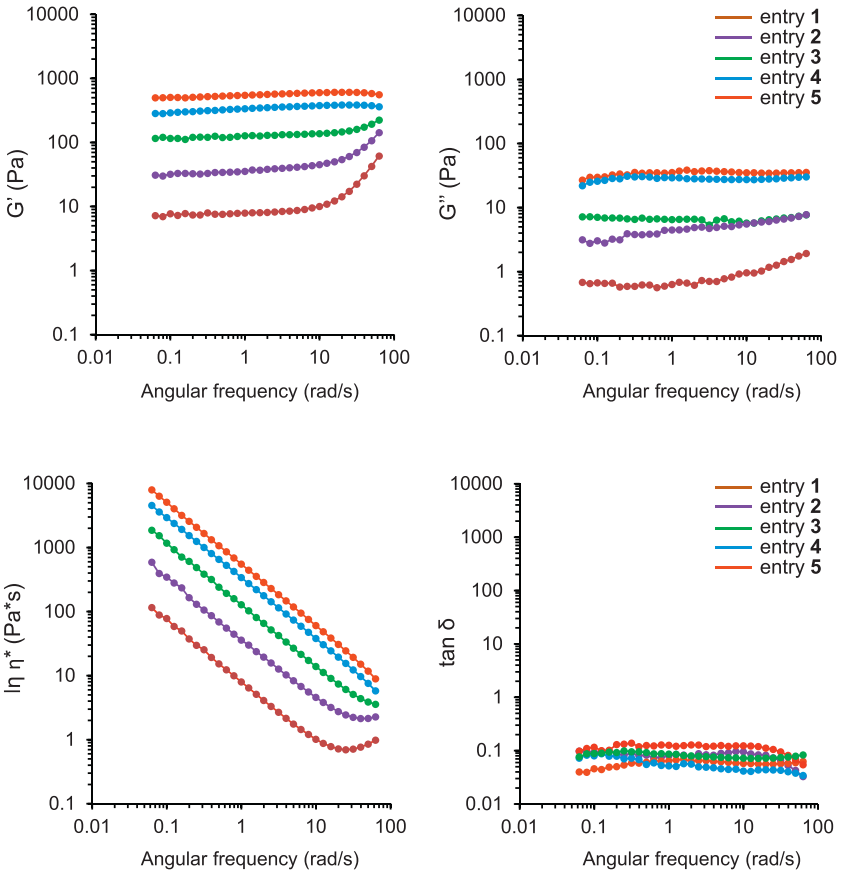

Fig. 5. Viscoelastic behavior of CMC hydrogels swelled with pure water (weight was 50 times its dry weight). This measurement was performed at 298 K.

loose structure of entry **3** could also hold water molecules inside of the gel as compared to the highly developed structure of entry **5** where $n_{PEG} = 36.3 \times 10^{-3}$. In the case of entry **1** whose n_{PEG} was 6.4×10^{-3}, a porous structure in the cross-section surface could not be observed, and thus the structure could not retain water inside of the gel, thereby resulting in the low water absorbency and low water-holding capacities.

3.5. Rheological properties

As shown in Fig. 5, the rheological moduli, tan δ, and η^* of the CMC hydrogels exhibited similar tendencies during the angular frequency sweeps. The storage modulus (G′) was always higher than the less modulus (G″) and there were no cross-over points (tan $\delta = 1$) for any of the hydrogels, indicating that the hydrogels had the characteristic gel structure because zero shear viscosity was not detected (Bhattarai, Ramay, Gunn, Matsen, & Zhang, 2005). In addition, tan δ was in the range 0.02–0.2, indicating that the elastic properties were superior to the viscous properties in the dynamic viscoelastic behavior of the CMC hydrogels. As seen in Fig. 5, the G′ of entries **4** and **5** exhibited almost no dependence on the frequency characteristic of a permanent gel network. In the case of entry **3**, the G′ value decreased by about 1 order of magnitude, but showed hardly any change in frequency dependence with respect to the strong gel. On the other hand, G′ of entries **1** and **2** showed drastic changes in the frequency dependence over 10 rad/s, indicating that entries **1** and **2** take the viscoelastic behavior of a weak gel (Argüelles-Monal, Goycoolea, Peniche, & Higuera-Ciapara, 1998). From these observations, it could be clarified that the viscoelastic behaviors of hydrogels strongly depended on the n_{PEG} of the hydrogels, and that the addition of a large amount of PEGDE to the reaction mixture to produce CMC hydrogels caused a significant increase of the moduli and η^*.

3.6. Cellulase degradability

Enzymatic degradation of the CMC hydrogels was performed at 40 °C using cellulase. The time dependence of degradation is shown in Fig. 6. After 3 days of incubation with cellulase, 62, 58, 47, 33, and 28% of CMC was found to be degraded in the hydrogels (entries **1–5**), respectively, under the conditions employed. The degradation speed as well as degradability decreased with

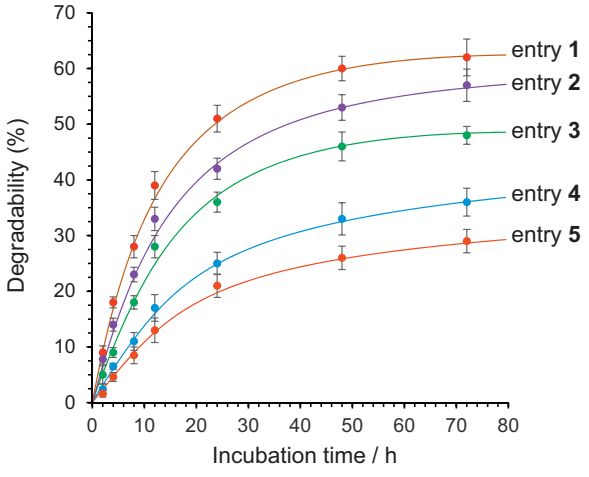

Fig. 6. Time-dependency of the degradability of CMC hydrogels by cellulase.

increasing n_{PEG} of the hydrogels, and no relation to the water absorbency (Fig. 3) or water-holding capacity (Fig. S6) could be observed.

3.7. Protein adsorption and release

In the protein adsorption and release experiments, hen egg white lysozyme and BSA were used as model proteins. The molecular weight and stokes' radius of lysozyme are 14 kDa and 2.1 nm, and those of BSA are 66 kDa and 3.4 nm (Batas, Jones, & Chaudhuri, 1997). Fig. 7 shows the adsorption of lysozyme and BSA to each hydrogel after 24 h, respectively. In all of the investigated cases, the amount of BSA adsorbed to the hydrogels was lower than that of lysozyme. In addition, the amount of adsorbed protein decreased with an increasing n_{PEG} and was not related to the absorbency of the hydrogels.

Next, protein release from the hydrogels determined after the adsorption experiments was performed in the same buffer solutions, as shown in Fig. 8. The protein release rates of both proteins rose with increasing n_{PEG} of the hydrogels. The release profiles exhibited a fast release rate in the first 10 h, followed by a virtually linear release over a 60 h period. In the initial release step until 10 h, hydrogels (entries **1**–**3**) released about 70% of the loaded proteins while over 40 and 50% of the loaded proteins remained in the gel structure of entries **4** and **5**, respectively.

The release rate of lysozyme was slightly different from that of BSA in all hydrogels. The release rate of BSA was slightly slower as compared to that of lysozyme in all cases, which suggests that the hydrogel structure, especially the pore size of network structure, influenced the protein release as well as adsorption. As shown in Fig. 4, the highly-crosslinked hydrogel exhibited a well-developed porous structure while the less crosslinked had less of a porous structure. The large pore size enhanced the protein adsorption and the release rates, while the small pore size suppressed the protein adsorption and the release rate due to the high crosslinking degree of hydrogels. In addition, since BSA has a large Mw and stokes' radius as compared to those of lysozyme, it could be considered that the amount of BSA adsorbed by the hydrogel and release rate of BSA were lower than those of lysozyme. From these observations, highly crosslinked hydrogels such as entries

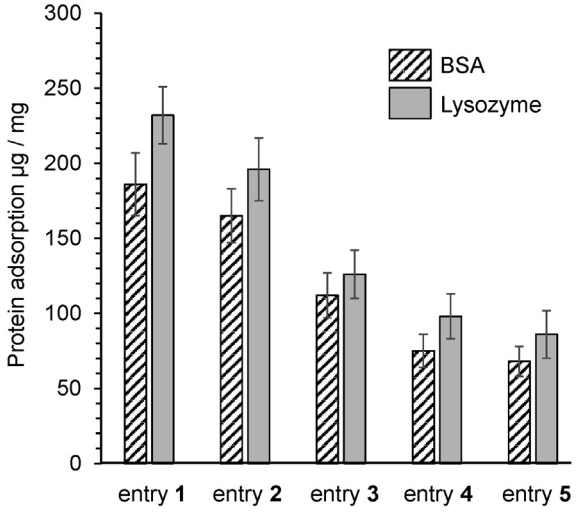

Fig. 7. Protein adsorption onto CMC hydrogels in lysozyme- or BSA-containing buffer solutions after 24 h.

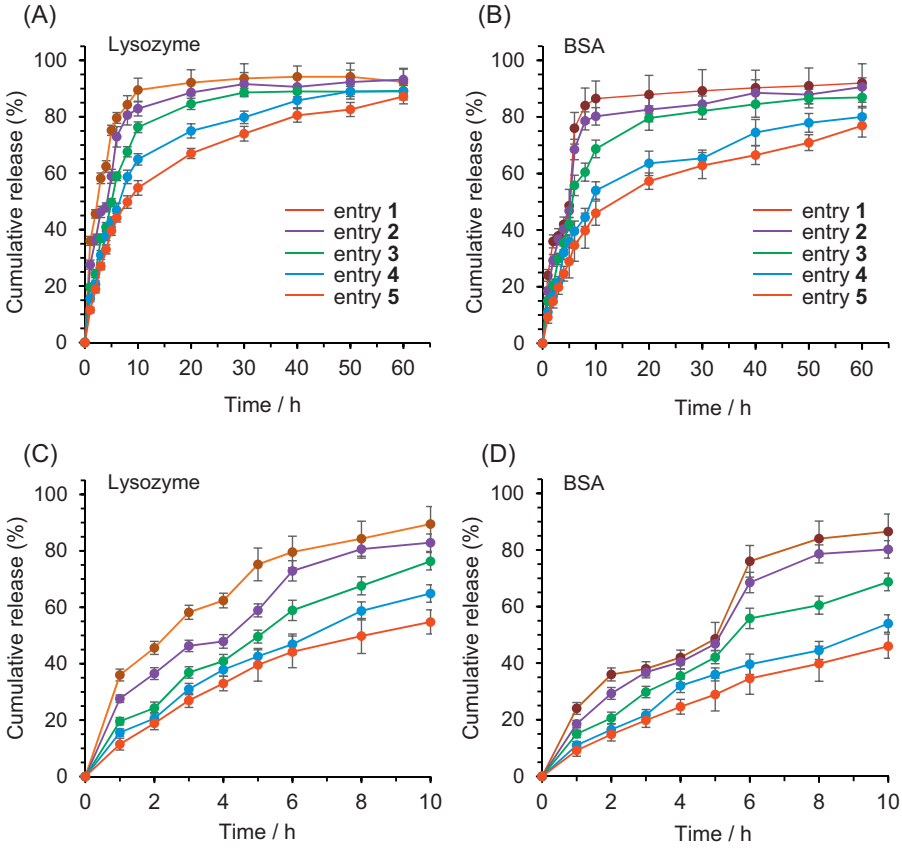

Fig. 8. Protein release profile from (A) lysozyme- or (B) BSA-adsorbed CMC hydrogels in buffer solutions, and expansion of the initial release profiles of the (C) BSA- and (D) lysozyme-adsorbed hydrogels.

4 and **5** are potentially suitable for long-term drug release applications, and the amount of loaded proteins and release rate are dependent on the molecular weight as well as the molecular size of proteins.

Regarding the interaction between proteins and ionic hydrogels, recent reports have revealed that BSA adsorptions toward amphoteric hydrogels prepared from chitosan include both electrostatic and hydrophobic interactions, and that the electrostatic interaction is mainly attributed to the ionization states of amino and carboxyl side chains of BSA within the protein structure and the hydrogel (Kono et al., 2013b). The pH of the protein adsorption medium is therefore considered to be a very important factor in determining the interaction between proteins and hydrogels, because the ionic states of the protein and hydrogel depend on pH of the medium (Denizli, Salih, & Pişkin, 1997; Denizli, Köktürk, Yavuz, & Pişkin, 1999). When the pH of the medium is greater than the isoelectric point (pI) of a protein, the protein molecule exhibits a negative charge. Conversely, when the pH of the medium is less than the protein pI, the protein exhibits a positive charge. In cases where the pH of the adsorption medium is approximately equal to the protein pI, hydrophobic interactions between the protein and hydrogel predominate, because the protein exhibits almost no electrical charge. In this study, 20 mM PBS buffer (pH 7.4) was used as the adsorption medium for lysozyme and BSA. Because the pI values of lysozyme and BSA are 10.5 (Stevens, 1991) and 4.7 (Yon, 1972), respectively, lysozyme and BSA were positively and negatively charged in the PBS buffer, respectively. Conversely, it was proposed that the CMC hydrogel was negatively charged because the pK_a of the carboxymethyl groups in CMC is around 4.3 (Tian et al., 2006), suggesting that there was an electrostatic attraction between BSA and the CMC hydrogel, while an electrostatic repulsion occurred between lysozyme and the CMC hydrogel. However, the amount of adsorbed lysozyme was higher than that of the adsorbed BSA in all the adsorption experiments for CMC hydrogels (Fig. 7), although there were also hydrophobic interactions between CMC hydrogel and BSA, and CMC hydrogel and lysozyme. This conflict suggests that interactions—except for electrostatic interactions—between CMC hydrogels and such proteins are influenced by the protein size, the structure of the CMC hydrogel, and especially the pore size. The effect of CMC hydrogel structures on the interaction between proteins and the CMC hydrogel was confirmed by protein release profiles (Fig. 8); increases in the n_{PEG} of CMC hydrogels caused the release rates for BSA and lysozyme to decrease. Therefore, the network structure—including crosslinking density and pore size—is also considered to determine the protein-adsorption and -release properties of the CMC hydrogels.

4. Conclusions

A biodegradable hydrogel was fabricated by chemically crosslinking PEGDE on CMC chains. The molar feed ratio of PEGDE to CMC in the preparation of the hydrogel strongly influenced the crosslinking degree of the obtained hydrogels. Water absorbency of the hydrogel depended on the crosslinking degree: lower crosslinking degrees could not retain water molecules inside the gel, whereas a higher degree of crosslinking suppressed the expansion of the gel structure. In addition, increase in the degree of crosslinking of the hydrogels was shown to lead to a decrease in biodegradability, similar to those of other cellulose derivatives. It was also shown to lead to an increase in physical strength of the hydrogels. The hydrogels also exhibited good adsorption abilities toward BSA as well as lysozyme. The proteins showed favorable drug release profiles: after an initial short burst release, virtually linear release profiles were obtained for the both proteins. These unique properties might enable the use of the hydrogels as drug delivery carriers for protein-based drugs if the biological safety of the hydrogel can be verified.

Acknowledgments

This work was supported in part by Grants-in-Aid for Scientific Research C-25410134 from the Japan Society for Promotion of Science (JSPS), and Grants-in-aids for the Adaptable and Seamless Technology Transfer Program through Targetdrive R&D (241FT0160 and AS242Z03384M) and Grants-in-aids for the Promoting Patent Licensing form Universities and Public Research Institutions to Industries from Japan Science and Technology Agency (JST).

Appendix A. Supplementary data

Supplementary data associated with this article can be found, in the online version, at http://dx.doi.org/10.1016/j.carbpol.2014.02.020.

References

Akar, E., Antinişk, A., & Seki, Y. (2012). Preparation of pH- and ionic-strength responsive biodegradable fumaric acid crosslinked carboxymethyl cellulose. *Carbohydrate Polymers*, *90*, 1634–1641.

Ali Hebeish Hashem, M., Abd El-Hady, M. M., & Sharaf, S. (2013). Development of CMC hydrogels loaded with silver nano-particles for medical applications. *Carbohydrate Polymers*, *92*, 407–413.

Argüelles-Monal, W., Goycoolea, F. M., Peniche, C., & Higuera-Ciapara, I. (1998). Rheological study of the chitosan/glutaraldehyde chemical gel system. *Polymer Gels and Networks*, *6*, 429–440.

Bailey, F. E., Jr., & Koleske, J. V. (1976). *Poly(ethylene oxide)*. New York: Academic Press.

Bailey, F. E., Jr., & Koleske, J. V. (1991). *Alkylene oxides and their polymers*. *Surfactant Science Series* (vol. 35) New York: Marcel Dekker.

Batas, B., Jones, H. R., & Chaudhuri, J. B. (1997). Studies of the hydrodynamic volume changes that occur during refolding of lysozyme using size-exclusion chromatography. *Journal of Chromatography A*, *766*, 109–119.

Bhattarai, N., Ramay, H. R., Gunn, J., Matsen, F. A., & Zhang, M. (2005). PEG-grafted chitosan as an injectable thermosensitive hydrogel for sustained protein release. *Journal of Controlled Release*, *103*, 609–624.

Canet, D. (1976). Systematic errors due to improper waiting times in heteronuclear Overhauser effect measurements by the gated decoupling technique. *Journal of Magnetic Resonance*, *23*, 361–364.

Chang, C., Duan, B., Cai, J., & Zhang, L. (2010). Superabsorbent hydrogels based on cellulose for smart swelling and controllable delivery. *European Polymer Journal*, *46*, 92–100.

Colombo, P., Bettini, R., Sabti, P., & Peppas, N. A. (2000). Swellable matrices for controlled drug delivery: gel-layer behaviour, mechanisms and optimal performance. *Pharmaceutical Science & Technology Today*, *3*, 198–204.

Craig, D. Q. M. (2002). The mechanisms of drug release from solid dispersions in water-soluble polymers. *International Journal of Pharmaceutics*, *231*, 131–144.

Denizli, A., Salih, B., & Pişkin, E. (1997). Comparison of metal chelate affinity sorption of BSA onto dye/Zn(II)-derived poly(ethylene glycol dimethacrylate-hydroxyethyl methacrylate) microbeads. *Journal of Applied Polymer Science*, *65*, 2085–2093.

Denizli, A., Köktürk, G., Yavuz, Y., & Pişkin, E. (1999). Albumin adsorption from aqueous solutions and human plasma in a packed-bed column with Cibacron Blue F3GA-Zn(II) attached poly(EGDMA-HEMA) microbeads. *Reactive & Functional Polymers*, *40*, 195–203.

Fuertges, F., & Abuchowski, A. (1990). The clinical efficacy of poly(ethylene glycol)-modified proteins. *Journal of Controlled Release*, *11*, 139–148.

Fung, B. M., Khitrin, A. K., & Ermolaev, K. (2000). An improved broadband decoupling sequence for liquid crystals and solids. *Journal of Magnetic Resonance*, *142*, 97–101.

Harris, J. M. (1985). Laboratory synthesis of polyethylene glycol derivatives. *Journal of Macromolecular Science, Part C: Polymer Reviews*, *25*, 315–324.

Kono, H. (2013). ^{1}H and ^{13}C chemical shift assignment of the monomers that comprise carboxymethyl cellulose. *Carbohydrate Polymers*, *97*, 384–390.

Kono, H., & Fujita, S. (2012). Biodegradable superabsorbent hydrogels derived from cellulose by esterification crosslinking with 1,2,3,4-butanetetracarboxylic dianhydride. *Carbohydrate Polymers*, *87*, 2582–2588.

Kono, H., Fujita, S., & Oeda, I. (2013). Comparative study of homogeneous solvents for the esterification crosslinking of cellulose with 1,2,3,4-butanetetracarboxylic dianhydride and water absorbency of the reaction products. *Journal of Applied Polymer Science*, *127*, 478–486.

Kono, H., & Nakamura, T. (2013). Polymerization of β-cyclodextrin with 1,2,3,4-butanetetracarboxylic dianhydride: synthesis, structural characterization, and

bisphenol A adsorption capacity. *Reactive and Functional Polymers*, *73*, 1096–1102.
Kono, H., Oeda, I., & Nakamura, T. (2013). The preparation, swelling characteristics, and albumin adsorption and release behaviors of a novel chitosan-based polyampholyte hydrogel. *Reactive and Functional Polymers*, *73*, 97–107.
Kono, H., Onishi, K., & Nakamura, T. (2013). Characterization and bisphenol A adsorption capacity of β-cyclodextrin-carboxymethylcellulose-based hydrogels. *Carbohydrate Polymers*, *98*, 784–792.
Kono, H., & Zakimi, M. (2013). Preparation, water-absorbency, and enzyme-degradability of novel chitin- and cellulose/chitin-based superabsorbent hydrogels. *Journal of Applied Polymer Science*, *128*, 572–581.
Lin, O. H., Kumar, R. N., Rozman, H. D., & Noor, M. A. M. (2005). Grafting of sodium carboxymethyl cellulose (CMC) with glycidyl methacrylate and development of UV curable coatings from CMC-*g*-GMA induced by cationic photoinitiators. *Carbohydrate Polymers*, *69*, 57–69.
Miller, G. L., Blum, R., Glennon, W. E., & Burton, A. L. (1960). Measurement of carboxymethylcellulase activity. *Analytical Biochemistry*, *1*, 127–132.
Nerurkar, N. L., Elliott, D. M., & Mauck, R. L. (2010). Mechanical design criteria for intervertebral disc tissue engineering. *Journal of Biomechanics*, *43*, 1017–1030.
Nilsson, M. (2009). The DOSY Toolbox: a new tool for processing PFG NMR diffusion data. *Journal of Magnetic Resonance*, *23*, 361–364.
Nishinari, K., Koyama, K., Williams, P. A., Phillips, G. O., Burchard, W. D., & Ogino, K. (1991). Solution properties of pullulan. *Macromolecules*, *24*, 5590–5593.
Rodŕiguez, R., Alvarez-Lorenzo, C., & Concheiro, A. (2003). Cationic cellulose hydrogels: kinetics of the cross-linking process and characterization as pH-/ion-sensitive drug delivery systems. *Journal of Controlled Release*, *86*, 253–265.
Rozenberg, M., Loewenschuss, A., & Marcus, Y. (1998). IR spectra and hydration of short-chain polyethyleneglycols. *Spectrochimica Acta Part A: Molecular and Biomolecular Spectroscopy*, *54*, 1819–1826.
Saha, N., Saarai, A., Roy, N., Kitano, T., & Saha, P. (2011). Polymeric biomaterial based hydrogels for biomedical applications. *Journal of Biomaterials and Nanobiotechnology*, *2*, 85–90.
Sannino, A., Demitri, H., & Madaghiele, M. (2009). Biodegradable cellulose-based hydrogels: design and applications. *Materials*, *2*, 353–373.
Stevens, L. (1991). Egg white proteins. *Comparative Biochemistry and Physiology Part B: Comparative Biochemistry*, *100*, 1–9.
Tian, F., Sandler, N., Gordon, K. C., McGoverin, C. M., Reay, A., Strachan, C. J., et al. (2006). Visualizing the conversion of carbamazepine in aqueous suspension with and without the presence of excipients: a single crystal study using SEM and Raman microscopy. *European Journal of Pharmaceutics and Biopharmaceutics*, *63*, 326–335.
Torchilin, V. P. (2002). PEG-based micelles as carriers of contrast agents for different imaging modalities. *Advanced Drug Delivery Reviews*, *54*, 235–252.
Ugwoke, M. I., Kaufmann, G., Verbeke, N., & Kinget, R. (2000). Intranasal bioavailability of apomorphine from carboxymethylcellulose-based drug delivery systems. *International Journal of Pharmaceutics*, *202*, 125–131.
Viel, S., Capitani, D., Mannina, L., & Segre, A. (2003). Diffusion-ordered NMR spectroscopy: a versatile tool for the molecular weight determination of uncharged polysaccharides. *Biomacromolecules*, *4*, 1843–1847.
Wester, P. W., van der Heijden, C. W., Bisschop, G. J., & van Esch, G. J. (1985). Carcinogenicity study with epichlorohydrin (CEP) by gavage in rats. *Toxicology*, *36*, 325–339.
Working, P. K., Newman, M. S., Johnson, J., & Cornacoff, B. (1997). Safety of polyethylene glycol) and poly(ethylene glycol) derivatives. In J. M. Harris, & S. Zalipsky (Eds.), *Polyethylene glycol chemistry and biological applications* (pp. 45–57). Washington, DC: American Chemical Society.
Yang, S., Fu, S., Liu, H., Zhou, Y., & Li, X. (2011). Hydrogel beads, based on carboxymethyl cellulose for removal heavy metal ions. *Journal of Applied Polymer Science*, *119*, 1204–1210.
Yon, R. J. (1972). Chromatography of lipophilic proteins on adsorbents containing mixed hydrophobic and ionic groups. *Biochemical Journal*, *126*, 765–767.
Zalipsky, S. (1995). Functionalized poly(ethylene glycols) for preparation of biologically relevant conjugates. *Bioconjugate Chemistry*, *6*, 150–165.
Zor, T., & Selinger, T. (1996). Linearization of the Bradford protein assay increases its sensitivity: theoretical and experimental studies. *Analytical Biochemistry*, *236*, 302–308.